J|A|C|S
ARTICLES
Published on Web 05/16/2006

Magnetic Resonance Imaging of the Manipulation of a Chemical Wave Using an Inhomogeneous Magnetic Field

Robert Evans,[†,‡] Christiane R. Timmel,[†,‡] P. J. Hore,[‡] and Melanie M. Britton*[,§,⊥]

Contribution from the Department of Chemistry, University of Oxford, Inorganic Chemistry Laboratory, South Parks Road, Oxford OX1 3QR, U.K., Department of Chemistry, University of Oxford, Physical and Theoretical Chemistry Laboratory, South Parks Road, Oxford OX1 3QZ, U.K., Magnetic Resonance Research Centre, Department of Chemical Engineering, University of Cambridge, New Museums Site, Pembroke Street, Cambridge CB3 2RA, U.K., and School of Chemistry, University of Birmingham, Edgbaston, Birmingham B15 2TT, U.K.

Received February 3, 2006; Revised Manuscript Received April 6, 2006; E-mail: m.m.britton@bham.ac.uk

Abstract: The effects of applied magnetic fields on the traveling wave formed by the reaction of (ethylenediaminetetraacetato)cobalt(II) (Co(II)EDTA^{2-}) and hydrogen peroxide have been studied using magnetic resonance imaging (MRI) . It was found that the wave could be manipulated by applying pulsed magnetic field gradients to a sample contained in a vertical cylindrical tube in the 7.0 T magnetic field of the spectrometer. Transverse field gradients decelerated the propagation of the wave down the high-field side of the tube and accelerated it down the low-field side. This control of the wave propagation eventually promoted the formation of a finger on the low-field side of the tube and allowed the wave to be maneuvered within the sample tube. The origin of these effects is rationalized by considering the Maxwell stress arising from the combined homogeneous and inhomogeneous magnetic fields and the magnetic susceptibility gradient across the wave front.

1. Introduction

Traveling waves have been observed in a variety of chemical reactions and result from a coupling between autocatalysis and diffusion.[1] Waves formed in these chemical systems provide an excellent opportunity to model biological wave formation, such as in chemotaxis and calcium waves. One such wave-forming reaction occurs between (ethylenediaminetetraacetato)-cobalt(II) (Co(II)EDTA^{2-}) and hydrogen peroxide, at pH 4.[2] Hydroxide ions autocatalyze this reaction, in which cobalt(II) is oxidized to cobalt(III) according to:

$$2\text{Co(II)EDTA}^{2-} + \text{H}_2\text{O}_2 \rightarrow 2\text{Co(III)EDTA}^{-} + 2\text{OH}^{-} \quad (1)$$

A chemical wave is produced by introducing hydroxide ions in a localized region of the reactive Co(II)EDTA^{2-}/H_2O_2 solution. Propagation of the wave occurs as the autocatalyst diffuses to neighboring regions. During the reaction, paramagnetic Co(II) ions are oxidized to diamagnetic Co(III) ions, and it is this difference, in the magnetic properties of reactants and products, that enables the wave to be observed using magnetic resonance imaging (MRI).[3] The NMR relaxation times of protons in water molecules surrounding the paramagnetic Co(II) ions are significantly shorter than for those surrounding diamagnetic Co-(III) ions, and this difference in relaxation times produces the image contrast necessary to visualize the traveling wave.

The transition from paramagnetic to diamagnetic cobalt produces a magnetic susceptibility gradient across the wave front. This, in conjunction with the associated concentration gradient, is responsible for the magnetic field effects observed for this wave in the presence of an inhomogeneous magnetic field.[3,4] In experiments conducted in a vertical tube, a descending wave produced chemical fingers.[3] Once a finger had formed, the velocity of the wave could be manipulated by applying a magnetic field gradient vertically along the length of the tube. For negative gradients, corresponding to a magnetic field larger at the top of the tube than at the bottom, an acceleration of the propagating finger was measured. Conversely, a slight decrease in the velocity of the wave was measured for positive gradients.[3] The origin of these observations was discussed in terms of the action of the Maxwell force, $\mathbf{F}_M = (V/\mu_0)\Delta\chi_V(\mathbf{B}\cdot\nabla)\mathbf{B}$ on a drop of one solution surrounded by another where $\Delta\chi_V$ is the difference in volume magnetic susceptibilities of the two solutions, μ_0 is the vacuum permeability, V is the volume of the drop, and $\mathbf{B}$ is the applied magnetic field vector. Therefore,

[‡] Department of Chemistry, University of Oxford, Physical and Theoretical Chemistry Laboratory.
[§] Magnetic Resonance Research Centre, Department of Chemical Engineering, University of Cambridge.
[⊥] School of Chemistry, University of Birmingham.
[†] Department of Chemistry, University of Oxford, Inorganic Chemistry Laboratory.

(1) Epstein, I. R.; Pojman, J. A. *An Introduction to Nonlinear Chemical Dynamics*; Oxford University Press: Oxford, 1998.
(2) Yalman, R. G. *J. Phys. Chem.* **1961**, *65*, 556.
(3) Evans, R.; Timmel, C. R.; Hore, P. J.; Britton, M. M. *Chem. Phys. Lett.* **2004**, *397*, 67.
(4) Boga, E.; Kádár, S.; Peintler, G.; Nagypál, I. *Nature* **1990**, *347*, 749.

the Maxwell force per unit volume for a drop of Co(III)EDTA$^-$ solution surrounded by Co(II)EDTA^{2-} solution is 2.1 N m^{-3}, for which $\Delta\chi_V = 0.184 \times 10^{-5}$.[3]

In our earlier experiments,[3] the sample was subjected to a longitudinal magnetic field gradient superimposed on the homogeneous magnetic field B_0 produced by the vertical superconducting magnet of the MRI spectrometer oriented along the axis (z) of the magnet bore, i.e., $B_z = B_0 + zG_z$, where $B_0 = 7.0$ T and $G_z = \partial B_z/\partial z = \pm 0.2$ T m^{-1}. In the work presented here, *transverse* gradients are applied to create a field $B_z = B_0 + yG_y$, where $G_y = \partial B_z/\partial y = \pm 0.2$ T m^{-1} and -2 mm $< y <$ 2 mm. Thus, the magnetic field in the z-direction varies in a linear fashion *across* the cylindrical sample tube rather than along its length.

In this paper, MRI has been used to follow the formation and propagation of the traveling wave formed in the reaction between Co(II)EDTA^{2-} and hydrogen peroxide. Descending traveling waves were initiated in vertical tubes, inside the MRI spectrometer. By applying linear transverse field gradients, the wave could be directed as it propagated downward, and the formation of a chemical finger could be forced. By switching the orientation of the transverse gradients the tip of the finger could be maneuvred.

2. Experimental Section

Sodium hydroxide, EDTA, cobalt(II) chloride, and hydrogen peroxide (35% solution by volume), all of A.C.S. grade, were obtained from Aldrich and were used without further purification. Solutions of 0.02 M Co(II)EDTA^{2-} were prepared by dissolving equimolar quantities of EDTA and $CoCl_2$ in deionized water and adjusting the pH to 4.0. The reacting solution was made from 0.02 M Co(II)EDTA^{2-} and hydrogen peroxide solutions, in a 9:1 ratio. The concentration of sodium hydroxide solution used to initiate the traveling wave was 0.016 M.

The reaction was studied in a 5 mm NMR tube and the wave initiated inside the spectrometer magnet, using a delivery device to introduce a drop of the sodium hydroxide solution on top of the Co(II)EDTA^{2-}/H_2O_2 solution. MRI experiments were performed on a Bruker DMX-300 spectrometer equipped with a 7.0 T superconducting magnet, operating at a proton resonance frequency of 300 MHz. All MRI experiments were carried out at a temperature of 22 $\pm$ 0.2 °C. The tube was imaged using a 25 mm radio frequency coil, which had a maximum vertical observational region of 30 mm.

Characterization of the reacting solution and experimental details can be found elsewhere.[3] Images were obtained using the fast imaging, multiple spin−echo sequence, RARE.[5] The orientations of images are shown in Figure 1. The *zy* images had a slice thickness of 1 mm and were positioned in the center of the tube. The vertical and horizontal fields of view were 50 and 12.5 mm, respectively. The corresponding pixel size was 195 μm × 195 μm. Multiple-slice experiments, which collected either six or ten *xy* images, were also acquired. Each slice had a thickness of 1 mm and separation of 1.2 mm and was composed of a 64 pixel × 64 pixel array with a field-of-view of 5 mm in both directions. The T_2 relaxation time of the Co(III)EDTA$^-$ solution was sufficiently long[3] that an image could be obtained from a single signal acquisition, so that the imaging time was 1 s for the *zy* images and 3 s for the *xy* multiple-slice images.

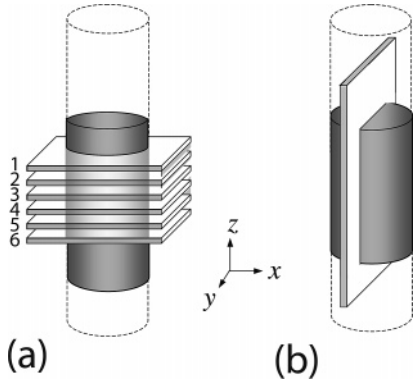

Figure 1. Schematic diagrams indicating image orientation and fields-of-view for multiple *xy* slices (a) and a *zy* slice (b). In both diagrams the gray area represents the field-of-view, which is the region of the tube held within the radio frequency coil.

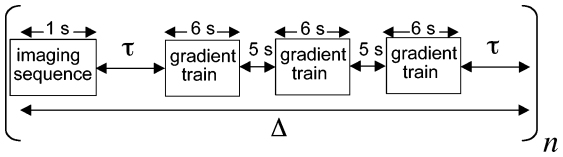

Figure 2. Schematic representation of the timings of imaging sequences and gradient trains, which are looped n times. The time value τ varies from 11 to 30 s, depending on the experiment. Δ is the time between imaging experiments.

To follow the effect of magnetic field gradients on the traveling wave, trains of gradient pulses were applied between image acquisitions. Gradient trains were generated using the imaging gradients of the spectrometer and comprised pulses which were switched on for 2 ms and off for 1 ms, cycled 2000 times, with amplitude of $+0.2$ T m^{-1} or -0.2 T m^{-1}. This produced an average gradient of ± 0.133 T m^{-1} over a period of 6 s. Constant gradients were not applied, as they could have damaged the gradient coils. Three gradient trains were applied, at 5 s intervals, between imaging experiments (Figure 2). Relatively long time intervals between images were chosen to minimize the influence on the wave from the magnetic field gradients involved in the *imaging* sequence. For negative gradients, the field (B_z) decreased from right to left across the sample/image and increased for positive gradients. Heating of the sample due to the imaging sequence and gradient pulses was negligible.

3. Results

In Figure 3 a series of typical *zy* images are shown over a period of approximately 7 min following wave initiation. Once the reaction was initiated at the top of the Co(II)EDTA^{2-}/H_2O_2 solution by adding a drop of NaOH solution, a traveling wave formed, which propagated downward, initially with a flat, horizontal interface. After a time, the wave front distorted and a finger formed. The propagation of this finger was faster than that of the flat wave front, and it is believed that this enhancement of the wave velocity is associated with convection. In these experiments, where no magnetic field gradients were applied except for those required for the imaging, the horizontal position at which the finger developed was found to be random,

(5) Hennig, J. *J. Magn. Reson.* **1988**, *78*, 397.

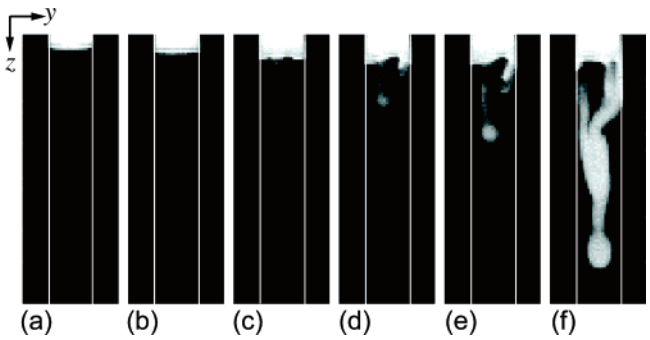

Figure 3. Time series of six MRI *zy* images of a traveling wave formed in the reaction of Co(II)EDTA^{2-} with H_2O_2. The slice thickness of each image is 1 mm, and a region of 45 mm (vertical) × 16 mm (horizontal) is displayed. Image (a) is taken 127 s after the wave was initiated by the addition of a drop of NaOH solution. Subsequent images were taken 186 s (b), 264 s (c), 318 s (d), 342 s (e), and 415 s (f) after initiation. Signal intensity is high (bright) where Co(III)EDTA$^-$ ions predominate and low (dark) where Co(II)EDTA^{2-} ions predominate. The vertical white lines in each image indicate the sides of the NMR tube.

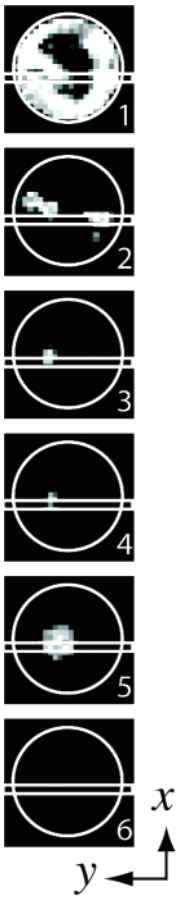

Figure 4. Multiple *xy* slice images taken through the length of a chemical finger formed 333 s after wave initiation. Each image has a slice thickness of 1 mm, with a separation of 1.2 mm between images, and a field of view of 5 mm in both *x* and *y* directions. Slice position 1 is the highest and is positioned close to the wave initiation position. The multiple-slice experiment for these images was performed between the *zy* images shown in d and e of Figure 3. The rectangle indicates the corresponding position of the *zy* images, and the circle represents the edge of the tube.

and frequently a second finger was formed. Figure 4 shows a series of six *xy* images taken between the two *zy* images shown in d and e of Figure 3. The rectangular box in Figure 4 indicates the slice position for the *zy* images (Figure 3d,e). The *xy* images

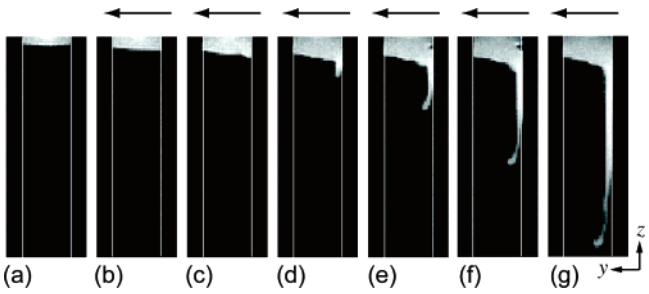

Figure 5. Time series of seven MRI *zy* images; parameters are the same as in Figure 3. Image (a) is taken 165 s after the wave was initiated by the addition of a drop of NaOH solution. Following image (a) magnetic field gradient trains were applied between imaging experiments, with a time delay, τ, of 11 s between gradient trains and imaging experiments. Applied gradients were in the $+y$ direction with the magnetic field increasing from right to left, as indicated by the arrow. Images were collected every 51 s and shown at 267 s (b), 369 s (c), 471 s (d), 522 s (e), 573 s (f), and 624 s (g) after wave initiation.

depicted here are acquired over a period of 3 s and show more fully the three-dimensional (3D) structure of the finger.

By applying magnetic fields which vary horizontally across the sample according to $B_z = B_0 + yG_y$ prior to finger formation, it was discovered that the propagating wave could be directed and the position of the finger controlled. In Figure 5, a series of *zy* images are shown where, after the first image, trains of positive *y* gradients are applied between imaging experiments, during which the magnetic field is greater on the left side than on the right side. The images are taken at 51 s intervals, with the first image taken 165 s following wave initiation.

The progress of the wave can be more clearly followed using the graph shown in Figure 6. The displacements of the wave front along the two dashed vertical lines shown in Figure 6a are plotted against time. Initially no gradients are applied, and the displacement of the wave is matched on both sides of the tube. From a point 178 s after wave initiation, a series of gradient trains are applied between images (as shown by the schematic in Figure 6b). A finger is formed on the right-hand side of the tube (the region of low field) 470 s after wave initiation (Figure 5d), and its propagation is significantly accelerated in contrast to the wave propagation on the left-hand side, which continues to proceed at the original velocity. Once the finger has formed, its velocity remains constant, in agreement with previous studies.[3]

To demonstrate that the finger develops in a fixed position and that no other fingers are formed outside of the central *yz* slice, six *xy* images were taken following trains of negative *y* gradient pulses, Figure 7. The horizontal slices clearly demonstrate that the finger forms in a specific, and fixed, position. The finger lies hard against the side of the tube, down its length, except for the tip or *leading-edge* which is located toward the center of the tube. The early part of the autocatalytic reaction takes part in this region of the finger.

We have observed that the position of finger formation is perfectly reproducible and dependent only on the direction of the applied *y* gradient. When positive *y* gradients are applied, and the magnetic field is at its greatest on the left side, the finger forms on the right side of the tube. In cases where a negative gradient is applied, the finger forms on the left side. With repeated application of these gradient trains additional fingers did not develop, in contrast to the situation in the absence of

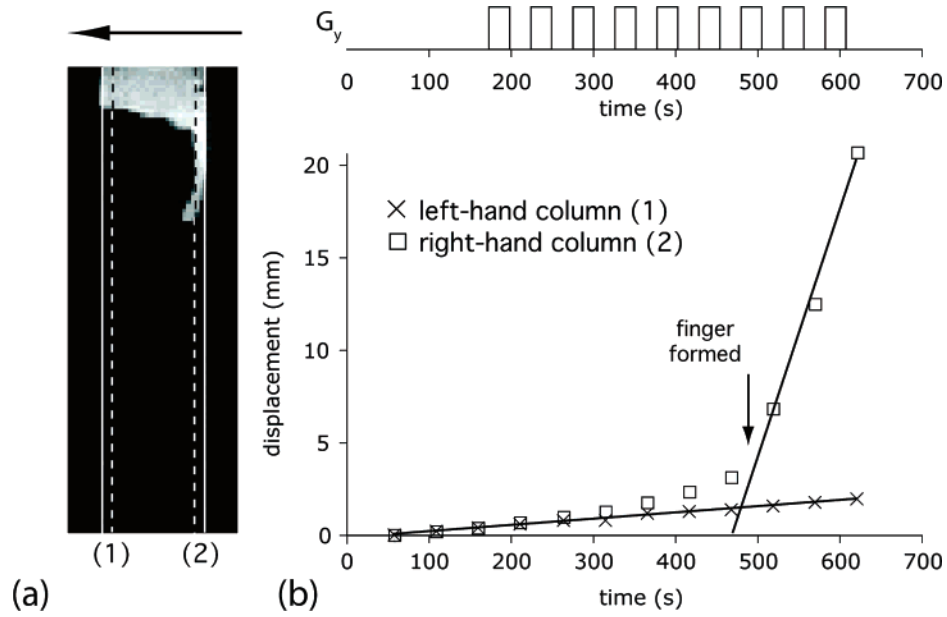

Figure 6. (a) MRI *zy* image of the chemical finger formed 573 s after wave initiation following the application of magnetic field gradient trains. Applied gradients were in the $+y$ direction with the magnetic field increasing from right to left. (b) Plot of chemical wave displacement against time along the two lines highlighted in the image in (a). Above the graph the timings for the gradient pulses are indicated, with respect to the data points.

the gradient pulses (Figure 3). However once a finger was formed, its position could be controlled by switching the direction of the magnetic field gradient. A typical example of this is shown in Figure 8. The first image is taken 20 s after the wave was initiated, prior to the application of the gradient pulse trains. The following two images are then taken following the application of a set of negative *y* gradient trains. The resulting finger is clearly seen in Figure 8c. Following this image the direction of the gradient train is switched and a train of positive *y* gradient pulses were applied. The position of the finger then clearly switches to the right side of the tube and continues to propagate down this side. It is important to note that only the tip of the wave is manipulated and the part of the finger containing the fully reacted $Co(III)EDTA^-$ solution remains fixed on the left side of the tube. Furthermore, a second finger starts to form on the right side of the tube from the interface at the top (Figure 8d).

Finally we observe that by rotating the direction of the magnetic field gradient in the *xy* plane, the tip of the chemical finger can be controllably positioned. To reduce the effect of the *imaging* gradients a limited number of slices was taken and so only a limited region of the finger could be observed by one set of *xy* images. To follow the rotation of the finger, slices were taken close to the finger tip as it propagated downward. In Figure 9 a set of *xy* images are shown of the part of the finger just above the tip, where it lies hard against the side of the tube, using B_z fields of the form $B_z = B_0 + (y \cos\theta\, G_y + x \sin\theta\, G_x)$, with $G_x = G_y$. The first image shows the orientation of the finger formed after a train of positive *y* gradient pulses. Subsequent images have trains of gradient pulses applied between imaging experiments which have been rotated by 45°. It can be seen that, as the gradient is rotated, so too is the position of the tip of the finger. As was seen in Figure 8, only the tip can be directed, and the fully reacted part of the finger remains fixed in position. So, as the finger propagates downward, the tip is rotated, thus creating a spiral down the length of the tube.

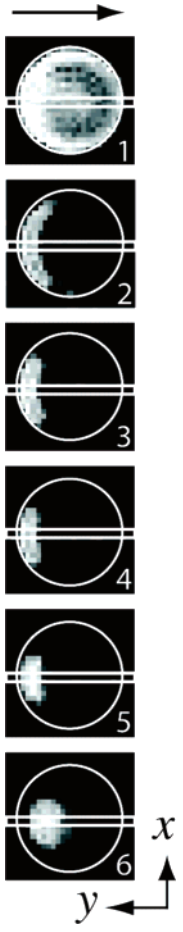

Figure 7. Multiple *xy* slice images taken through the length of a chemical finger formed 246 s after wave initiation following the application of magnetic field gradient trains. Applied gradients were in the $-y$ direction with the magnetic field increasing from left to right, as indicated by arrow. Each image has a slice thickness of 1 mm, with a separation of 1.2 mm between images, and a field of view of 12.5 mm in both *x* and *y* directions. Slice position 1 is the highest and is positioned near where the wave was initiated.

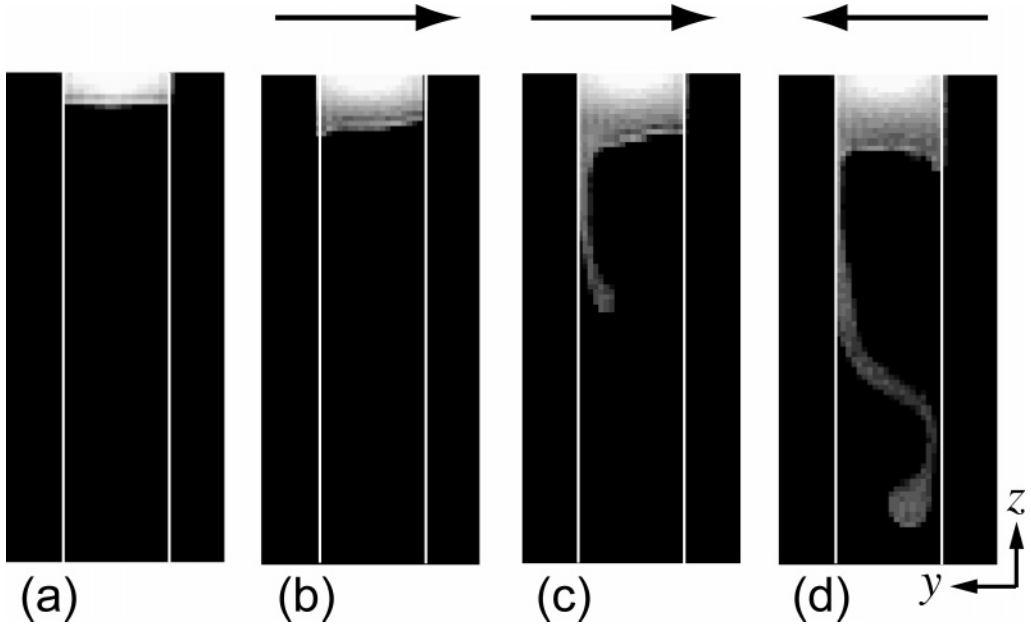

Figure 8. Series of MRI *zy* images; parameters are the same as in Figure 3. Image (a) was taken 20 s after wave initiation. Following image (a), magnetic field gradient trains were applied between imaging experiments and subsequent images were collected 71 s (b), 123 s (c), and 175 s (d) after wave initiation. For the images shown in (b) and (c) the applied gradients were in the $-y$ direction. Following image (c) the direction of the gradients were switched to $+y$. The arrows indicate the direction in which the magnetic field increases during the gradient trains, which were applied prior to acquiring the images.

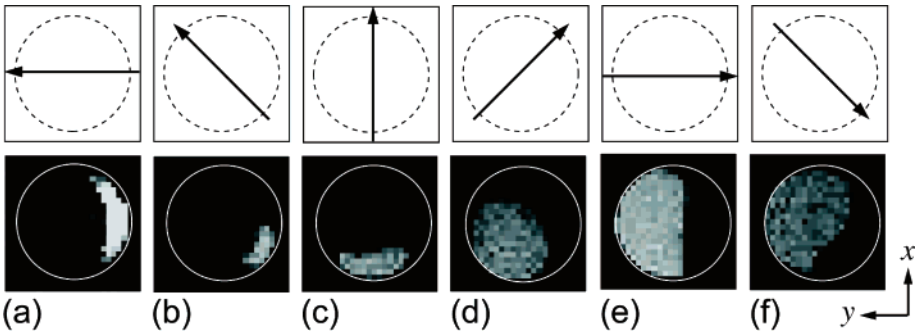

Figure 9. Time series of MRI *xy* images following the tip of the finger as it propagates downward. Gradient trains are applied between imaging experiments where the direction of the gradient is rotated in the *xy* plane. The arrows indicate the direction in which the magnetic field increases during the gradient trains, which were applied prior to acquiring the images. The position of each *xy* slice is moved to follow the part of the finger just above the tip, where it touches the wall of the tube. The positions of these slices, relative to the position of the chemical wave just after initiation, are 2.0 mm (a), 6.3 mm (b), 10.9 mm (c), 16.9 mm (d), 18.1 mm (e), 18.4 mm (f).

4. Discussion

In general terms, the Maxwell force is given by

$$\mathbf{F}_M = (V/\mu_0)\Delta\chi_V(\mathbf{B}\cdot\nabla)\mathbf{B} = \begin{pmatrix} F_x \\ F_y \\ F_z \end{pmatrix} = k\begin{pmatrix} B_x\partial B_x/\partial x + B_y\partial B_x/\partial y + B_z\partial B_x/\partial z \\ B_x\partial B_y/\partial x + B_y\partial B_y/\partial y + B_z\partial B_y/\partial z \\ B_x\partial B_z/\partial x + B_y\partial B_z/\partial y + B_z\partial B_z/\partial z \end{pmatrix} \quad (2)$$

where k is the collection of constants $(V/\mu_0)\Delta\chi_V$. Hence, for a force F_q to act on the wave in direction q, at least one term of the form $B_p\partial B_q/\partial p$ needs to be nonzero.

In the experiments reported by Evans et al.,[3] it was clear that the applied field, with its longitudinal gradient, $B_z = B_0 + zG_z$, produced a force in the z-direction:

$$F_z \propto B_z\partial B_z/\partial z = (B_0 + zG_z)G_z \approx B_0G_z \quad (3)$$

(using $B_0 \gg zG_z$). At first sight, however, it would appear that a transverse gradient superimposed on the spectrometer field, i.e., $B_x = B_y = 0$, $B_z = B_0 + yG_y$, as employed here, could have no effect on the wave propagation. For a field of this form, the only nonzero gradient is $\partial B_z/\partial y$ so that, from eq 2, $F_x = F_y = 0$, and $F_z = kB_yG_y = 0$, because there is no applied field in the y-direction.

However, in the absence of electric currents in the sample or time-dependent electric fields, Maxwell's equation, $\nabla \times \mathbf{B} = 0$, means that the following relation must hold:

$$\frac{\partial B_p}{\partial q} = \frac{\partial B_q}{\partial p},\ p,q = x,y,z \quad (4)$$

Consequently, when a magnetic field $B_z = B_0 + yG_y$ is applied to the sample, there *must* also be a "concomitant" field gradient in the y-direction: $B_y = zG_y$. Thus:

$$F_y \propto B_z\partial B_y/\partial z = (B_0 + yG_y)G_y \approx B_0G_y \quad (5)$$

(note that with $G_y = 0.2$ T m^{-1} and $|y| < 2$ mm, we have $yG_y \ll B_0$ and $F_z = kB_yG_y = kzG_y^2 \ll F_y$). These so-called concomitant magnetic fields are known to create a number of artifacts in MRI at low fields, particularly in experiments that

are sensitive to phase evolution.[6] In the work presented here the concomitant gradients generate no detectable artifacts of this type but are responsible for the ability to manipulate the wave using magnetic forces that are transverse to the direction of propagation.

Equation 5 clearly demonstrates that F_y is the dominant force component for this system and that it changes direction when the applied gradient is reversed. As shown in Figures 5−9, the sign of G_y determines the initial point of formation for the chemical finger as well as its consequent motion within the tube. As expected, the finger (of diamagnetic reaction product) is exclusively formed in the region of lowest field. Consequent application of magnetic field gradients allows the finger to be "pushed" around within the tube as the (diamagnetic) finger consistently moves toward the lowest field region of the tube.

Finally it is interesting to note that only the *leading-edge* of the finger is affected by the gradient trains. As seen in Figure 8, when the gradient direction is reversed during an experiment, only the most recently reacted part of the finger can be manipulated by the applied field. In contrast, regions of the finger that formed prior to switching the gradients remain unaffected. Possible explanations for this phenomenon might be based on the increased significance of hydrodynamic instabilities at the leading edge of the finger or on the curvature of the wave front. Further work is underway to investigate the origin of this effect.

By applying gradient pulse trains of variable direction spatial patterns such as spirals (Figure 9) can be set up within the tube. The design of such spatial patterns is presently limited by several factors: (i) it is only possible to manipulate the tip of the finger at its point of formation; (ii) the chemical reaction proceeds in all directions, and hence, the finger becomes blurred as the reaction proceeds (Figure 9d,e,f); (iii) the reaction cannot easily be driven "upwards" by an applied magnetic field gradient. In relation to the last point, Evans et al.[3] have shown that positive field gradients lead to a significant increase in the downward wave front velocity but negative field gradients retard the velocity to a smaller extent, presumably as a result of convection. Viscosity and concentration control of the reaction mixture and suppression of convection might allow even more dramatic magnetic manipulation of such wave reactions.

(6) Norris, D. G.; Hutchison, J. M. S. *Magn. Reson. Imaging* **1990**, *8*, 33.

5. Conclusion

It has been shown that the spatial evolution of a descending wave front, for the autocatalytic oxidation of Co(II)EDTA^{2-}, can be controlled by applying magnetic field gradients of suitable orientation. Both the position of finger formation and its consequent propagation direction can be controlled reproducibly by appropriately chosen magnetic field orientations. Maxwell stress can account for this observed behavior.

The experimental methods described in this paper are expected to be suitable for the manipulation of other traveling chemical waves. The prerequisite for the success of magnetically controlled spatial wave evolution is the existence of magnetic susceptibility gradients across the reaction boundary. The exciting possibility of controling polymer synthesis based on radical chain carriers is just one potential application of this technique at present under investigation.

Acknowledgment. M.M.B. thanks EPSRC for an Advanced Research Fellowship and Prof. L. F. Gladden and the MRRC, Cambridge University, for support. C.R.T. thanks the Royal Society for a University Research Fellowship and the EPSRC for financial support. We are grateful to Prof. R. J. Ordidge and Prof. G. A. Brooker for advice on concomitant field gradients.

JA0608287